Molecular Dynamics Simulations of the Structures of Alkane/Hydroxylated α-Al_2O_3(0001) Interfaces

Ryan Y. Jin,[†] Kihyung Song,[‡,§] and William L. Hase*[,‡]

Department of Chemistry and Department of Electrical and Computer Engineering, Wayne State University, Detroit, Michigan 48202

Received: August 19, 1999; In Final Form: January 4, 2000

Molecular dynamics simulations were carried out on several linear alkane systems of different chain lengths, confined between hydroxylated α-aluminum oxide surfaces at experimental densities, to study structural and dynamical features of the film/surface interfaces. The simulations show that there is extensive multilayer adsorption on the hydroxylated α-aluminum oxide surface. The adsorption layers are separated by the diameter of the linear alkanes, independent of chain length. Alkanes near the surface show a high percentage of the trans conguration as well as greater densities, indicating efficient packing of chains in the inner adsorption layer. The simulations indicate that this "solidification" increases as the alkane chain becomes longer. Radial distribution functions also show a more-ordered multilayer packing structure for alkane chains physisorbed on the surface as compared to the bulk. The dynamics of chains in the first adsorption layer are strongly affected by their interactions with the solid surface. Diffusion within this innermost layer is efficient, although there is negligible diffusion out of this layer on a 500-ps time scale. The surface also affects the diffusion dynamics of the second layer, but for the smaller alkanes the diffusion dynamics of the third and other, further-removed layers are the same as those for the bulk.

I. Introduction

Aluminum oxide (Al_2O_3) is a very important refractory ceramic material.[1,2] The aluminum oxide surface plays a significant role as a catalyst and catalyst support.[3,4] Modified forms of the alumina surface are used in analytical and separation processes.[5,6] Alumina in the forms of α- and γ-Al_2O_3 is also one of the main constituents of rocket exhaust formed by solid rocket motors.[7]

Because of its technological importance, numerous recent theoretical and experimental studies have addressed the properties of alumina and its surfaces. Experiments have probed the surface energies and relative stabilities of nanocrystalline aluminas;[8,9] the adsorption of water[8−11] and other molecules[12−16] on α-Al_2O_3(0001);[19,20] and the adhesive, frictional, and wear properties of alumina surfaces.[21,22]

A variety of theoretical approaches have been used to study alumina surfaces and interfaces of alumina with other materials. Empirical electrostatic potentials for alumina[23−26] have been used, in molecular dynamics simulations, to study energetic and structural properties of bulk alumina, alumina surfaces, and alumina interfaces.[24,27−34] Semiempirical,[35,36] density functional,[37,38] and ab initio[39−42] electronic structure theory calculations have been used to study the structures and energies of alumina surfaces and their interactions with water and other molecules.

Molecular dynamics simulations have been used to study liquid hydrocarbon adsorption[32,41] and subsequent water penetration[32] on an aluminum oxide surface. The alkane chains exhibited strong layering and densification in the direction parallel to the surface. These properties, which arise from the oriented interactions between the liquid molecules and the surface,[43−45] are similar to those of confined films. Considerable understanding of the latter has been obtained from experiments[46−53] probing liquid structure and forces at a molecular level and from atomistic computer simulations.[54−67] The computer simulations have given a molecular-level understanding of adhesion, packing structures, dynamics, and other details of confined films that cannot easily be achieved through experiment.

Confining a thin liquid film between surfaces induces changes in the structural features as well as dynamical properties of the liquid. Computer simulations show distinctive multilayering and oscillatory behavior of the layers, in terms of both density and solvation force.[65,66] The first liquid layer, in immediate contact with the surface, is intimately influenced by its interactions with the solid surface.[68] Furthermore, it was found that the wall-to-wall separation greatly affects the structure of the confined liquid.[69] In particular, as the separation of the two opposing surfaces increases above approximately 10 atomic diameters, the influences of the solid surfaces appear to diminish in the middle of the confined liquid, resulting in a central region where the behavior of the liquid closely resembles that of the bulk.[58] The computer simulations have also shown little difference in the behavior of the fluids when confined between structured and structureless solid surfaces.[69]

In this paper is presented a series of molecular dynamics simulations of the interfacial structures and dynamics of the straight-chain alkane liquids *n*-octane (C8), *n*-hexadecane (C16), and *n*-dotriacontane (C32) interacting with a hydroxylated α-Al_2O_3(0001) surface. Elucidation of the behaviors of such interfaces is of paramount importance to many practical problems, such as friction, lubrication, membrane contacts and separations, etc. Alkane chains of different lengths are inves-

[†] Departments of Chemistry and Electrical and Computer Engineering.
[‡] Department of Chemistry.
[§] On leave from the Department of Chemistry, Korea National University of Education, Chongwon, Chungbuk 363-791, Korea.

10.1021/jp992922y CCC: $19.00
Published on Web 03/02/2000

TABLE 1: Potential Functions and Parameters for V_{alkane} Bonded Interactions[a]

	potential functions	constants	
stretch	$V_s = {}^1/_2\, k_s(r - r_0)^2$	$k_s = 663$	$r_0 = 1.54$ Å
bend	$V_\theta = {}^1/_2\, k_\theta(\theta - \theta_0)^2$	$k_\theta = 482$	$\theta_0 = 111.6$
torsion	$V_\phi = {}^1/_2\, k_1[1 + \cos(\phi)]$ + ${}^1/_2\, k_3[1 + \cos(3\phi)]$	$k_1 = 3.35$	$k_3 = 13.4$

[a] Potentials are from ref 73. k_s and k_θ are in units of kJ/(mol·Å^2) and kJ/(mol·rad^2), respectively. Both k_1 and k_3 are in units of kJ/mol.

tigated in this study to determine how the adsorption of the alkane on the alumina surface is affected by its length. Simulations are also carried out for the corresponding bulk systems to contrast their results with those obtained in the presence of the hydroxylated alumina surface. The strength of the alkane/surface adsorption potential is varied to examine, in detail, its effect on the interfacial structure and dynamics.

II. Potential Energy Function

A rigid hydroxylated α-Al_2O_3(0001) surface was assumed for this study. The structure of the surface is based on ab initio calculations of hydroxylated alumina clusters that were used to represent the α-Al_2O_3(0001) surface.[40] The surface is terminated by a single layer of hydroxyl groups. The ab initio calculations indicate that there is very little relaxation of the hydroxylated alumina surface,[40] so the surface structure was assumed to be the same as that for the bulk.[70,71]

The potential energy function for the alkane/hydroxylated alumina systems studied here is written as

$$V = V_{alkane} + V_{alkane,alkane} + V_{alkane,surface} \quad (1)$$

V_{alkane} is the intramolecular potential for an alkane molecule, $V_{alkane,alkane}$ is the alkane−alkane intermolecular potential, and $V_{alkane,surface}$ is the interaction potential between an alkane molecule and the hydroxylated alumina surface. A united-atom (UA) model[72] was used to represent the CH_3 and CH_2 groups of the alkanes and the hydroxyl groups of the surface.

The UA model that was used for V_{alkane} has been used previously in simulations of bulk alkanes.[73,74] In this model, the CH_3 and CH_2 groups are treated equivalently, with UA stretch, bend, and torsion bonded potentials and with a Lennard-Jones 6-12 nonbonded potential. The bonded potential terms and their parameters are given in Table 1. The Lennard-Jones potential is given by

$$V(r_{ij}) = 4\epsilon\left[\left(\frac{\sigma}{r_{ij}}\right)^{12} - \left(\frac{\sigma}{r_{ij}}\right)^{6}\right] \text{ for } r_{ij} \le r_c$$

$$V(r_{ij}) = 0 \text{ for } r_{ij} > r_c \quad (2)$$

where r_{ij} is the distance between UA atoms i and j. r_c denotes the computational nonbonded spherical cutoff radius. The use of such a cutoff is standard in molecular dynamics simulations,[72] as it reduces the number of two-body interactions that must be evaluated and helps make many-atom and long-time simulations feasible. A value of 7 Å was used for r_c in these simulations. Similar values for r_c have been used in previous simulations of alkane systems.[73−76] A nonbonded potential was included between two UAs in an alkane chain separated by 4 or more UAs. The ϵ and σ parameters for $CH_2(CH_3)$ UAs are from the OPLS force field[77] and are given in Table 2.

The $V_{alkane,alkane}$ intermolecular potential is written as a sum of Lennard-Jones 6-12 potentials between the UAs for the two alkanes. The same ϵ and σ parameters and cutoff r_c are used as for V_{alkane}.

TABLE 2: Lennard-Jones UA Potential Parameters[a]

type	ϵ	σ
$CH_2(CH_3)\cdots CH_2(CH_3)$[b]	0.493	3.905
OH···OH	0.711	3.070
$CH_2(CH_3)\cdots$OH[b]	0.592	3.462
$CH_2(CH_3)\cdots$Al[c]	24.87	2.459
$CH_2(CH_3)\cdots$O[c]	0.209	3.608

[a] ϵ is in kJ/mol, and σ is in Å. [b] Potential parameters from ref 75. [c] Potential parameters from ref 41.

The $V_{alkane,surface}$ potential is given by a sum of Lennard-Jones 6-12 terms between the UAs of the alkanes and the UA hydroxyl groups and Al and O atoms of the surface. The same cutoff radius r_c of 7 Å was used for these potential terms as for the above V_{alkane}. The ϵ and σ parameters for an alkane UA/hydroxyl UA interaction were obtained from a geometric combination of OPLS force field values[75] of ϵ and σ for $(CH_3)CH_2\cdots CH_2(CH_3)$ and OH···OH UA interactions. High-level ab initio calculations for CH_4 interacting with $Al_{2n}O_{3n}$ clusters have been used to determine Lennard-Jones potentials for a $(CH_3)CH_2$ UA interacting with the Al and O atoms of an α-Al_2O_3(0001) surface.[41,42] Those potentials are used here, and all of the Lennard-Jones parameters for $V_{alkane,surface}$ are listed in Table 2.

For homogeneously distributed systems, an analytic correction term can be added to account for interactions beyond the r_c cutoff.[72] However, it was not possible to make such a correction to the systems studied here, because of the heterogeneity of the alkane/hydroxylated alumina interface.

The above Lennard-Jones potentials fitted to the $CH_4/Al_{2n}O_{3n}$ ab initio calculations give alkane/α-Al_2O_3(0001) adsorption energies[41,42] that are considerably larger than the reported experimental values.[12] For example, for octane/α-Al_2O_3(0001) the depth of the potential energy minimum from the Lennard-Jones potential is 326 kJ/mol, whereas the experimental 300 K desorption energy is 61.1 kJ/mol.[12] This large difference cannot be resolved by using larger $Al_{2n}O_{3n}$ clusters and higher levels of theory in the ab initio calculations.[42] However, because of the highly reactive nature of the Al-terminated α-Al_2O_3(0001) surface, small amounts of any contaminants will readily react with the surface and change its properties.[78] Any adherents on the surface are expected to have much weaker interactions with the alkane than do the small aluminum cations and, thus, to give rise to a much smaller adsorption energy. It is rather conspicuous that the desorption energies measured for the alkanes are nearly the same as the corresponding bulk heats of sublimination,[12] which suggests that the alkane may be interacting with an organic material on the surface or with an O-atom-terminated surface instead of with the small aluminum cations.

The potential energy functions in eqs 1 and 2, without the r_c cutoff and with the parameters in Tables 1 and 2, give 152, 296, and 565 kJ/mol, respectively, for the depths of the potential energy minima for *n*-octane, *n*-hexadecane, and *n*-dotriacontane adsorbed on the hydroxylated α-Al_2O_3(0001) surface. These potential wells are much shallower than those for the Al-terminated surface because the terminating hydroxyl groups increase the distance between the alkane and the surface aluminum atoms. As discussed above, because of the computational requirements for these simulations, a cutoff radius r_c of 7 Å was used for the Lennard-Jones (6-12) potential terms, which affects the alkane/hydroxylated alumina well depth. It reduces the well depths by ∼20−30% from the above values to 110, 230, and 464 kJ/mol for the C8, C16, and C32 alkanes, respectively. For each of the potential energy minima, the alkane lies trans-flat on the hydroxylated alumina surface.

Calculations were performed to determine how such modifications in the interaction potentials, between the $(CH_3)CH_2$ united atoms of the alkane and the aluminum and oxygen atoms of the alumina surface, affect properties of the alkane/hydroxylated alumina interface. In particular, the ϵ parameters for the $(CH_3)CH_2\cdots$Al and $(CH_3)CH_2\cdots$O interactions were each lowered to 43 and 21% of the above values. For the interaction with Al cation, the values of the ϵ parameters become 10.66 and 5.33 kJ/mol, whereas the values become 0.090 and 0.045 kJ/mol for the interaction with the O atom. Lowering the ϵ parameters decreases the alkane adsorption energy. For the octane/hydroxylated α-Al_2O_3(0001) system, the depths of the adsorption potential energy minima become 64.2 and 48.5 kJ/mol, with the above decreases in the ϵ parameters and a r_c cutoff radius of 7 Å. (Note that the interaction between the alkane UAs and the hydroxyl UA is not adjusted.) The 64.2-kJ/mol value for the potential energy minimum is similar to that of the experimental adsorption energy for the octane/α-Al_2O_3(0001) interface.[12]

III. Computational Procedure

A. Simulation Cell. The first step in generating our bulk, multiple-chain alkane system involved packing alkane chains in a large cubic box with periodic boundary conditions imposed in all directions. The dimension of the periodic box was adjusted and the system allowed to equilibrate to a densely packed bulk system with a volume appropriate to the corresponding experimental density. A confined alkane system was then generated by turning off the periodic boundary conditions in the *z* direction. Because the hydroxylated aluminum oxide surface employed in this study was impenetrable to the alkane chains, periodic boundary conditions were no longer valid in the *z* direction, so the chains had to be reconnected and the coordinates of their atoms translated into their true or "unwrapped" positions in the *z* direction. Two identical hydroxylated aluminum oxide surfaces were then placed, parallel to each other, at the sides of the box along the *z* direction, and the interaction potentials between the surfaces and alkanes were implemented. While periodic boundary conditions in the *x* and *y* directions were retained, the alkane systems were compressed as the distance between the two solid surfaces was decreased. The separation of the two surfaces was then adjusted until the target density was attained. The confined alkane system was then further equilibrated for 2 ns, with the dimensions of the periodic box in both the *x* and *y* directions kept constant at 25.0 or 35.0 Å (see discussion below).

As discussed below in section IV, the presence of the hydroxylated surface alters the structure of the liquid at the liquid/surface interface. To obtain the complete structure of the interface, it was necessary to use a sufficiently large simulation cell and a sufficiently large number of alkane chains so that the density and structure of the liquid in the middle of the cell approximated that of the bulk. For the C8, C16, and C32 liquids in the box with a 25 Å × 25 Å surface area, this result was obtained with 134, 70, and 50 alkane chains, respectively, and with respective separations between the two surfaces of 57.8, 54.2, and 73.2 Å.

B. Hydroxylated Alumina Surface. Most of the simulations were performed with a periodic box that had an $x-y$ surface area of 25 Å × 25 Å. This box was placed on a rigid hydroxylated α-Al_2O_3(0001) surface with a 46 Å × 46 Å, or 10 × 10 unit cell, area in the $x-y$ plane. This surface, depicted in Figure 1, is terminated by a single layer of 339 hydroxyl groups, represented by (OH) united atoms. The surface consists of (OH)−Al−Al−O−Al layers of atoms, where the distance from the top layer of the (OH) united atoms to the bottom layer of Al atoms is 3.05 Å. As discussed above in section II, the surface structure was assumed to be the same as that for the bulk.[70,71] The (OH)−Al, Al−Al, Al−O, and O−Al interlayer distances were 0.86, 0.47, 0.86, and 0.86 Å, respectively.

The above 25 Å × 25 Å box is not long enough in either the *x* or the *y* direction to contain the extended conformations of the C16 and C32 alkanes, which are the minimum energy structures of these molecules when they are interacting with the hydroxylated alumina surface. Thus, this periodic box does not simulate the complete interaction between the extended alkane and the interface. Previous work has shown that this is not a critical issue for simulating highly averaged properties for an interface with weak interactions, such as those between a glassy polymer and graphite.[79] However, to properly simulate detailed structural and dynamical properties of the highly heterogeneous alkane/hydroxylated alumina interface, which has much stronger interactions, it may be important to use a model with a surface area large enough to enclose the extended alkane.[32] Thus, simulations for the C16/hydroxylated alumina interface were also performed using a periodic box with an $x-y$ surface area of 35 Å × 35 Å, placed on a hydroxylated α-Al_2O_3-(0001) surface with a 70 Å × 70 Å, or 15 × 15 unit cell, area. This surface is terminated by a single layer of 734 hydroxyl united atoms. A periodic box large enough to contain the extended C32 alkane was not used in this work, because of the computational requirements for such a simulation, and detailed properties are not reported for the C32/hydroxylated alumina interface.

C. Molecular Dynamics Simulations. The computer program used for the work presented here was developed from a general molecular dynamics computer program that was used in previous simulations of bulk polymeric systems.[73,74] The simulations reported here were carried out under conditions of fixed particle number, constant volume, and constant temperature (NVT).[72] Temperature was controlled via Berendsen's method,[80] in which constant temperature is achieved by exchanging energy between the system and an external heat bath. The classical equations of motion were integrated with the velocity Verlet algorithm,[81] using a time step of 1 fs. A typical simulation required 500 000−1 000 000 time steps, or 0.5−1 ns. Coordinates and velocities of the particles were accumulated for every 1000 or 2000 time steps (1 or 2 ps). Most of the computations were carried out on an SGI dual-processor Octane workstation.

IV. Results and Discussion

A. Density Profile. A snapshot of the simulation for the *n*-octane/hydroxylated alumina system is shown in Figure 2. Apparent from this figure is a layered structure at the liquid/solid interface. Quantitative features of this interface can be determined from the density profile $\rho(z)$, which gives the density of a particular particle (such as an atom) at a perpendicular distance *z* from the surface, that is,

$$\rho(z) = \frac{dN(z)}{dz} \tag{3}$$

where $N(z)$ is the number of particles at distance *z*.

Density profiles for the C8, C16, and C32 systems at 300 K are shown in Figure 3. The data shown were averaged over 500 or 1000 frames of trajectories. Multilayer adsorption on the aluminum oxide surfaces can readily be seen for each of

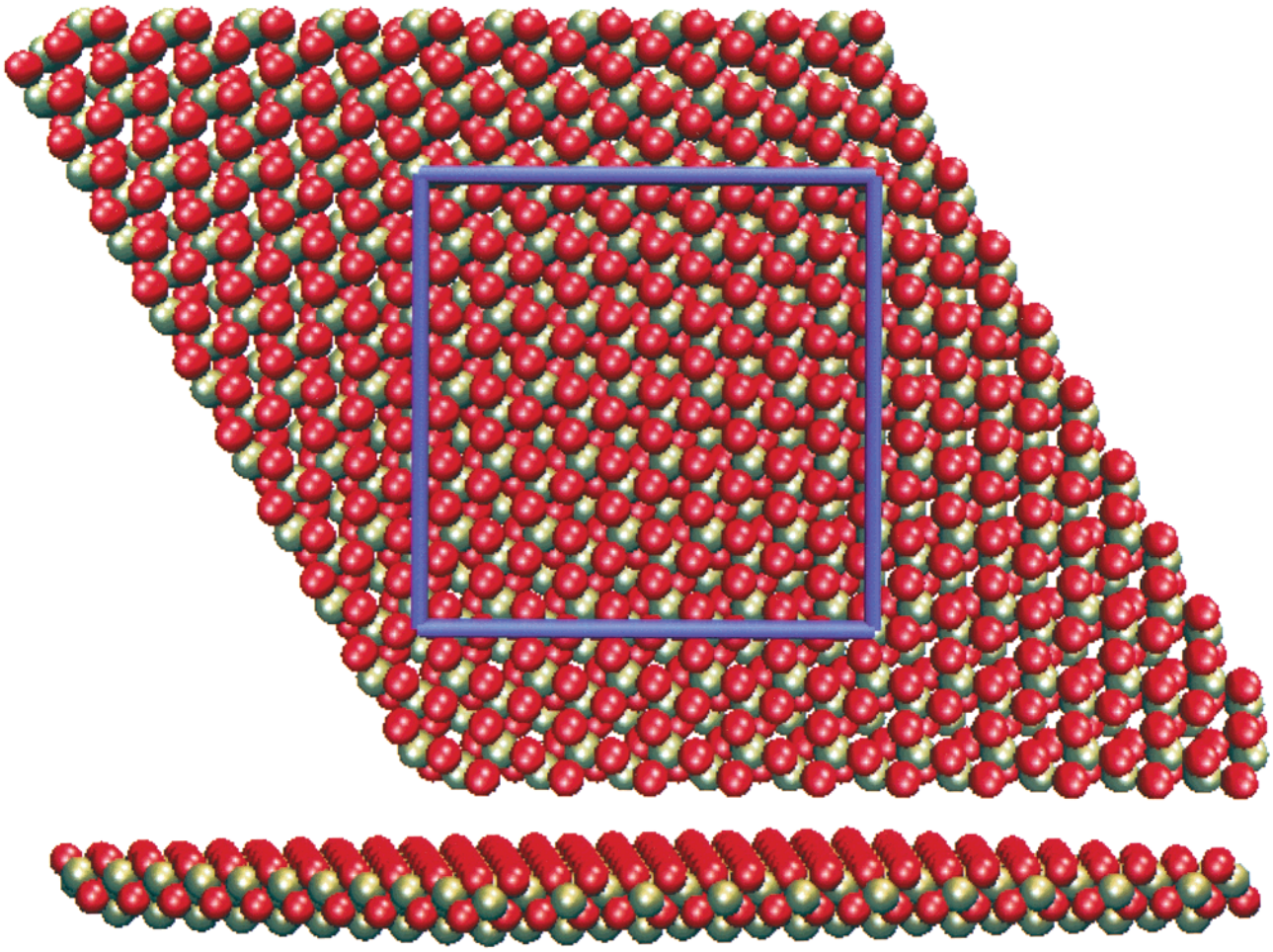

Figure 1. Top and side views of the hydroxylated α-Al_2O_3(0001) surface, with a 46 Å × 46 Å, or 10 × 10 unit cell, area in the $x-y$ plane. The 25 Å × 25 Å periodic box placed on this surface is denoted by the solid blue line. The OH united atoms and O atoms are red, and the aluminum atoms are gold.

the alkane systems, with five well-identified adsorption layers. For each of the systems, the adsorption peaks are at the same distances from the surface and are approximately the same heights, which indicates that the density profile of the interface is independent of the length of straight-chain alkanes.

The first peak in the density profile is approximately 3 Å from the surface, which agrees with the equilibrium separation for the nonbonded van der Waals interaction between the UA $CH_2(CH_3)$ group and the UA hydroxyl group. The distance separating the first, second, and subsequent layers is found to be approximately 4.5 Å. The average positions $\bar{z}_n$ of the two peaks in the density profile for these layers are computed according to

$$\bar{z}_n = \frac{z_n + (h - z_n')}{2} \tag{4}$$

where z_n and z_n' represent the locations of the two peaks away from the surfaces and h is the separation distance between the two solid surfaces. The results are shown in Figure 4, where the positions of the peaks are plotted versus peak number. The same linear curve for the three systems indicates consistency of the spacings between successive layers. A slope of 4.5 Å is obtained for this line, which represents the average separation between the layers. This distance is in good agreement with the distance between two $CH_3(CH_2)$ UAs at their nonbonded potential energy minimum, which is 4.38 Å.

The presence of the surface has the strongest effect on the first layer, which has a density that is the most unlike the bulk value. The increased density at the interface and the decaying oscillatory behavior of the density profile have both been found in previous simulations for linear alkanes in the presence of a surface.[44,45,57,58,61−66] This layered structure is also observed in the solvation force. Monte Carlo and molecular dynamics[64−66] simulations of straight-chain alkanes confined between two surfaces have found that the solvation force oscillates with respect to the distance from the surface, with a peak-to-peak separation similar to the molecular diameter. Similarly, in surface force apparatus studies of linear alkane films between solid surfaces,[46,82] the shear force is found to oscillate with surface separation and with a periodicity comparable to the molecular diameter of a linear alkane molecule, independent of chain length.

Figure 3 shows that the layering at the liquid/surface interface extends for more than 25 Å from the surface, that is, for more than five diameters of the $CH_2(CH_3)$ UA. The transition to the bulk density after five oscillations (or layers) in the density profile agrees with previous simulations of straight-chain liquid alkanes confined between two surfaces.[44,45,57,58,64−66]

A simulation with a cell too small to show the transition from oscillatory layering to the bulk system shows only the inner layering at the interface. This is shown in Figure 5 for the C32 alkane, where the separation between the surfaces of the simulation cell is one-half the value for the density profile given

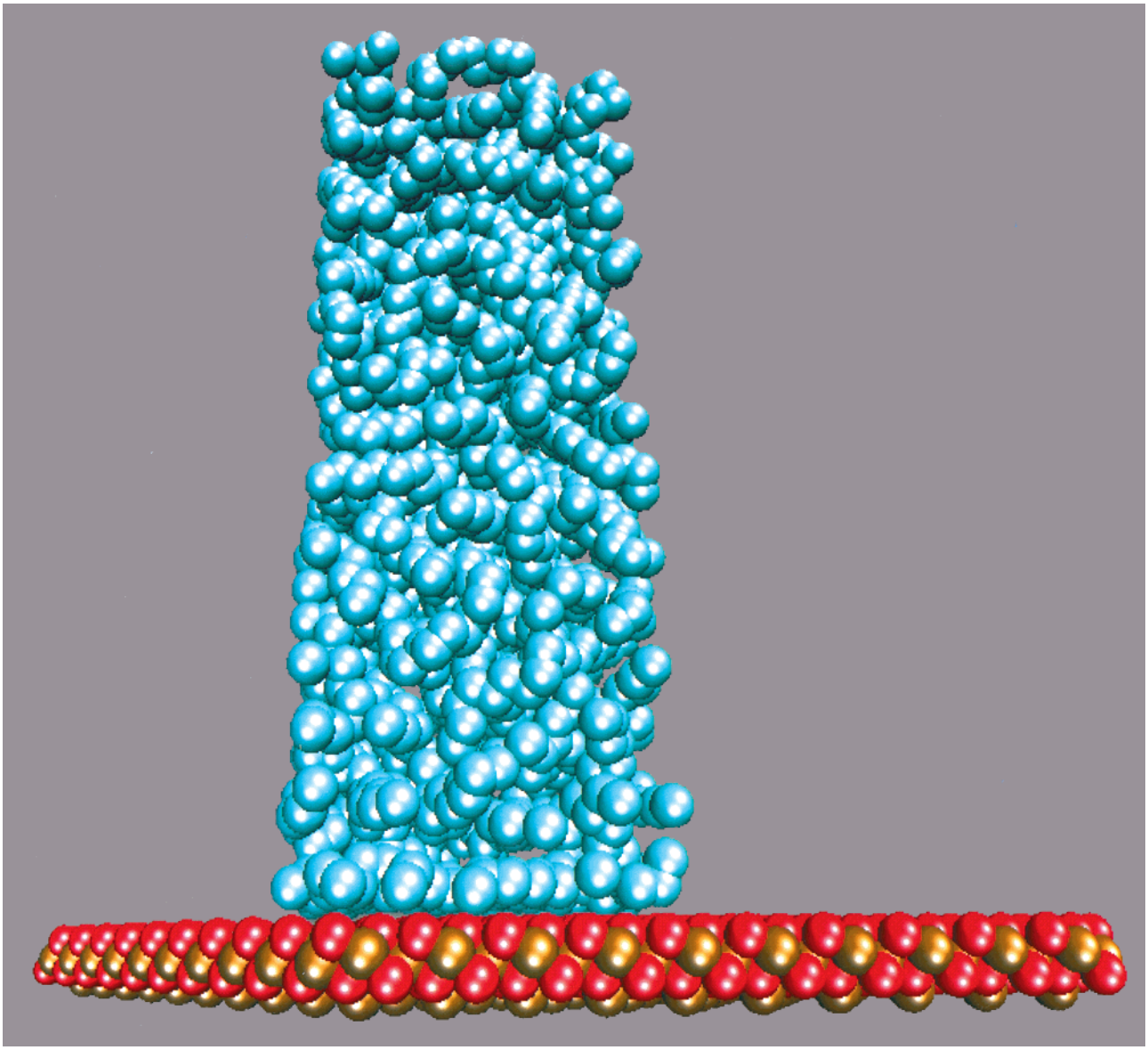

Figure 2. Snapshot of the molecular dynamics simulation for the *n*-octane/hydroxylated alumina system. Layering is seen at the interface.

in Figure 3 (that is, the number of alkane chains is also reduced by one-half). Figure 5 shows the same four inner layers, with nearly the same densities as found using the larger simulation cell.

B. Radial Distribution Function. Using the separation between layers determined above, the UAs of the alkane chains were assigned to specific layers, and UA−UA radial distribution functions (RDFs) were calculated for each layer. To assist in determining how the alkane/hydroxylated alumina interface affects the structure of the individual alkane chains and the interchain packing, the RDFs were partitioned into intramolecular and intermolecular contributions. The intramolecular RDFs for the first three layers of the octane/hydroxylated alumina system at 300 K are shown in Figure 6, where they are compared with that for the bulk. The principal structural features in these plots are the 1−3 couple (∼2.50 Å), the gauche 1−4 couple (∼3.25 Å), the trans−gauche 1−5 couple (∼4.50 Å), the trans−trans 1−5 couple (∼5.00 Å), the trans−trans−trans 1−6 couple (∼6.50 Å), and the trans−trans−trans−trans 1−7 couple (∼7.50 Å). The curves are "scaled" so that the height of the 1−3 couple is the same for each layer. An important feature of these plots is the increased number of trans conformations and the decreased number of gauche defects for the chains in the innermost layer, which is consistent with the trans-flat potential energy minimum structure for octane bound to the surface. For example, only for the inner layer is the trans−trans−trans−trans 1−7 couple readily apparent. This increased tendency for trans conformations does not extend beyond the inner layer. The RDFs for the second and third layers are similar to that for the bulk. A preference for adsorbed linear alkanes to adopt a trans conformation has been seen in previous simulations for alkane/Au[44] and alkane/alumina[32,41] interfaces.

The intramolecular RDFs for the C16/hydroxylated alumina system at 300 K are plotted in Figures 7 and 8 for a periodic box with a 25 Å × 25 Å and a 35 Å × 35 Å surface area, respectively. The RDFs in Figure 7 are similar to those in Figure 6 for octane. The inner layer has a larger number of trans conformations and a smaller number of gauche defects than does the bulk. The second and third layers have RDFs similar to that for the bulk. A comparison of the RDFs in Figures 7 and 8 shows that increasing the area of the periodic box to 35 Å × 35 Å, so that an extended *n*-hexadecane molecule can lie on the surface, significantly increases the extent of trans structure found in the innermost layer. Couples beyond 7.5 Å are clearly

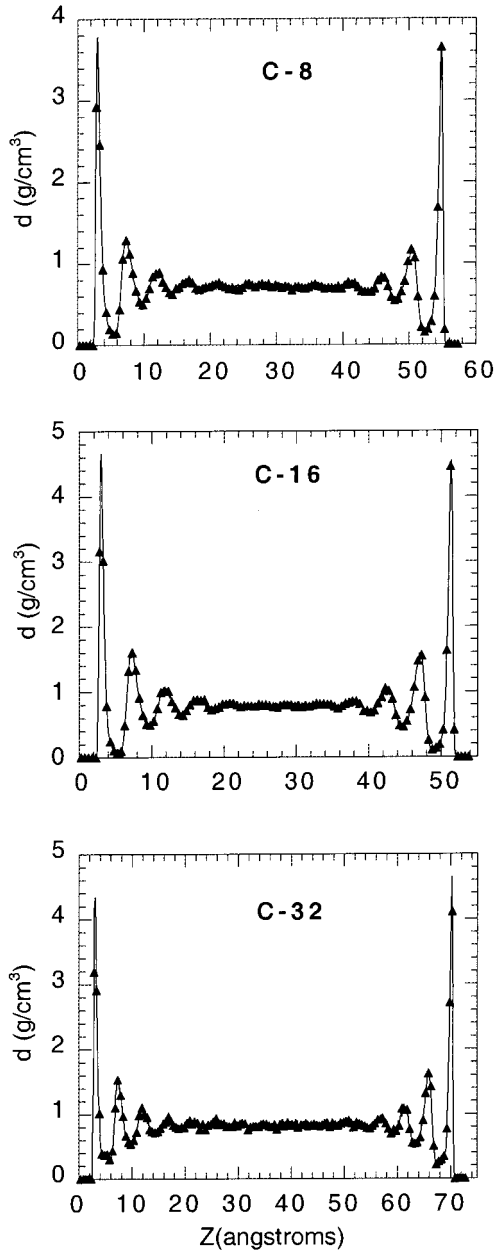

Figure 3. Density profiles of the *n*-octane (C8), *n*-hexadecane (C16), and *n*-dotriacontane (C32) alkanes between hydroxylated α-Al_2O_3(0001) surfaces at 300 K. The densities and structures of the alkanes in the middle approximate those of the bulk systems. The periodic box with the ×surface area of 25 Å × 25 Å was used for these simulations.

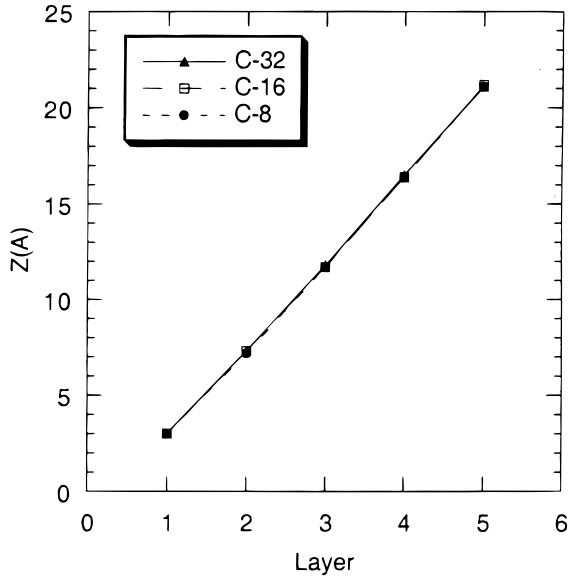

Figure 4. Peak positions from Figure 3 of the adsorption layers for interfaces of *n*-octane (C8), *n*-hexadecane (C16), and *n*-dotriacontane (C32) interacting with a hydroxylated α-Al_2O_3(0001) surface.

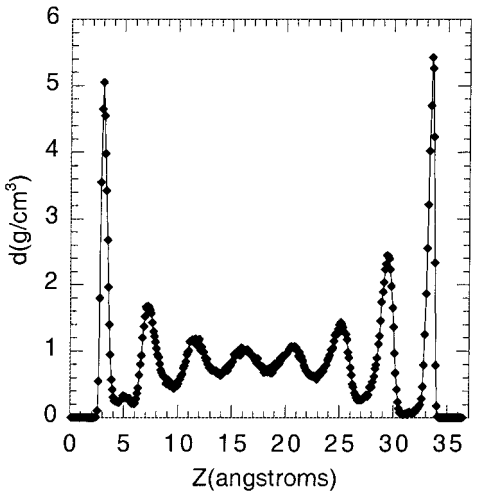

Figure 5. Same as Figure 3 for C32, except the simulation cell has one-half the distance between the surfaces.

evident, and there are negligible gauche defects. The RDF for the third layer is similar to that for the bulk; however, the second layer has a RDF with more trans conformations and fewer gauche defects. The simulations with the larger surface area suggest that C16 has more "solidification" at the interface than does C8, which is consistent with a higher melting point and stronger interaction with the surface for C16 than for C8. It would be of interest to use quite large boxes to simulate the detailed structure of C32 and even larger alkanes at the hydroxylated alumina interface.

C. Interfacial Dynamics. The mobility of the chains was studied by determining their *r* (that is, *x*, *y*, *z*) and *z* displacements versus time. The former reflects the total diffusion of the chain, whereas the latter reflects diffusion in the *z* direction, perpendicular to the surface. To determine these dynamics for the different layers, the r_i and z_i displacements of the centers of mass of chains initially in a particular layer were followed for 500 ps at 300 K, using the periodic box with the surface area of 25 Å × 25 Å. There were no diffusions out of the innermost layer for any of the three alkane systems. Diffusion did occur for the second and third layers. For the octane system, approximately 10% and 30% of the chains diffused out of the second and third layers, respectively. The extent of diffusion for the third layer, within this time frame, is similar to that for the same layer width in the bulk.

Although there was no diffusion out of the innermost layer, there was considerable diffusion within this layer. The average *r* (*x*, *y*, *z*) displacement of the chains in this layer is 3−4 Å for the C32 system, in contrast to the much smaller average *z* displacement of ∼0.9 Å. Both the average *r* and the average *z* displacements of the second and third layers of this system are similar to the bulk values of ∼6 and ∼2.5 Å, respectively.

The above results agree with those of previous simulations.[68,69] Toxvaerd[68] has found that the presence of the surface affects the dynamics of only the first layer and not those of layers further from the surface. Similarly, simulations of liquid-filled pores have shown that the average diffusion coefficient

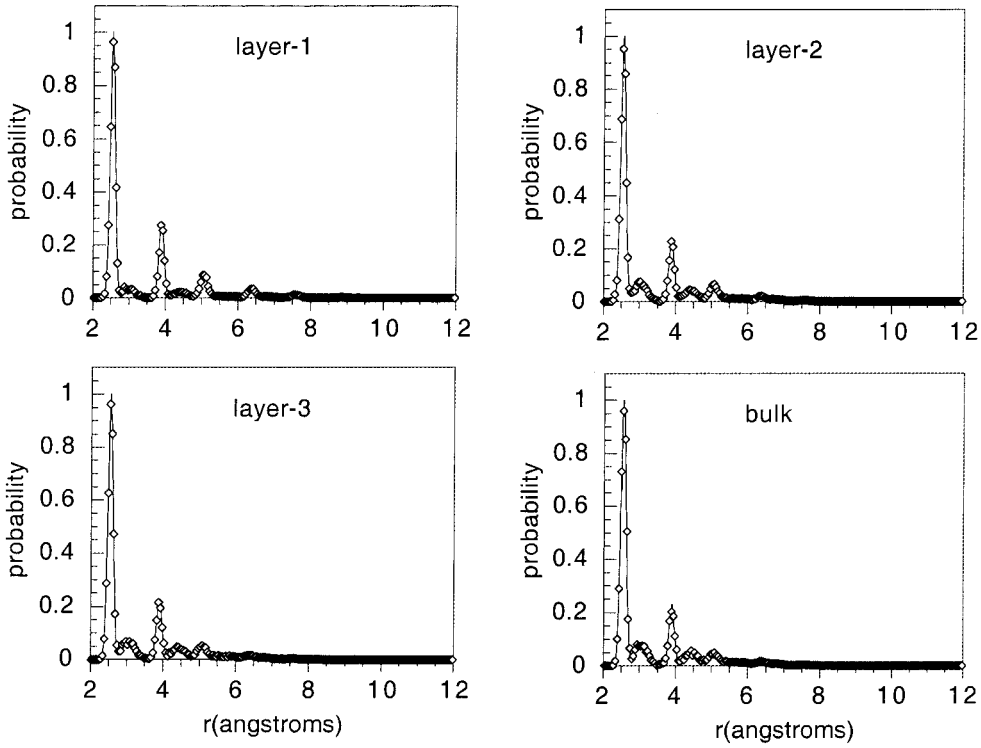

Figure 6. Comparison of intramolecular radial distribution functions for the first three layers of the C8/hydroxylated alumina system and for bulk C8. The curves are scaled so that the first peak, for the 1−3 couple, is the same height for all of the curves. The periodic box with the ×surface area of 25 Å × 25 Å was used for these simulations.

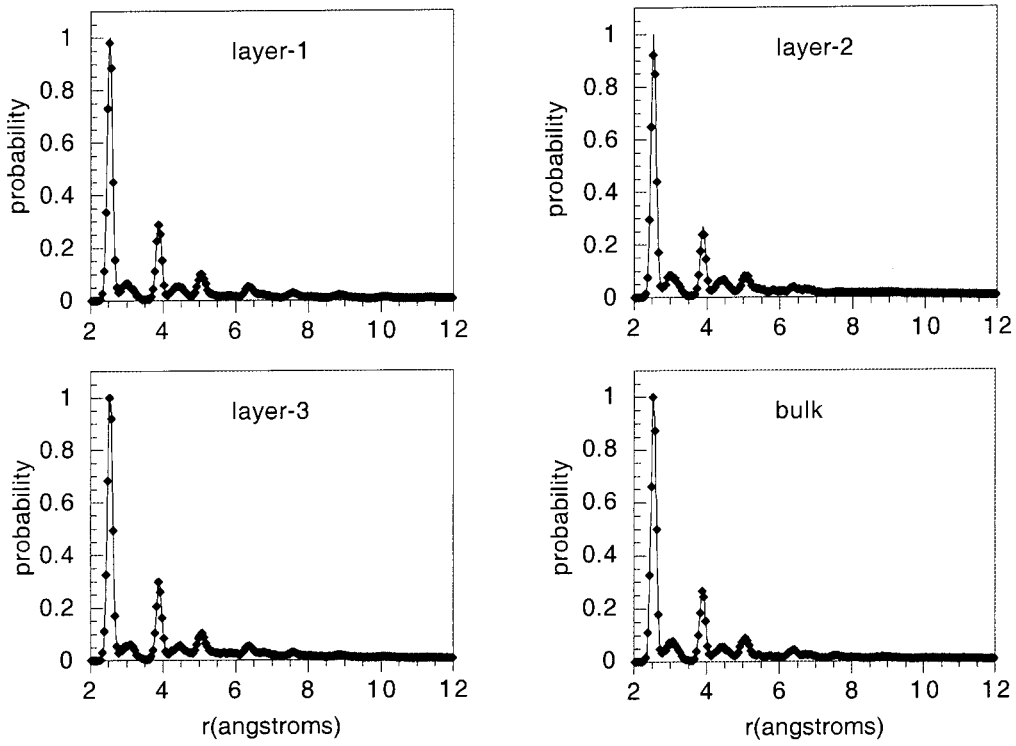

Figure 7. Same as Figure 6, but for the C16/hydroxylated alumina system.

in the center of the pore approaches the bulk value at a distance of more than 10 molecular diameters from the pore's surface.[69]

Strong interactions between the inner alkane layer and the surface are also evident in the trans ↔ gauche interconversion rate, as observed in previous studies for different systems.[65,66] This rate depends on local properties of the chain and is expected to be insensitive to the chain length and the size of the periodic box. For the C32 system, using the periodic box with the surface area of 25 Å × 25 Å, the trans ↔ gauche interconversion rate at 300 K is 0.35 bond^{-1} ps^{-1} for the inner layer and 3.1 bond^{-1} ps^{-1} for the bulk. The trans ↔ gauche interconversion rates for the second and third layers are statistically the same as that for the bulk.

In future work, it would be of interest to use sufficiently large periodic boxes to converge the diffusion properties of large alkane/hydroxylated alumina interfaces as a function of layer.

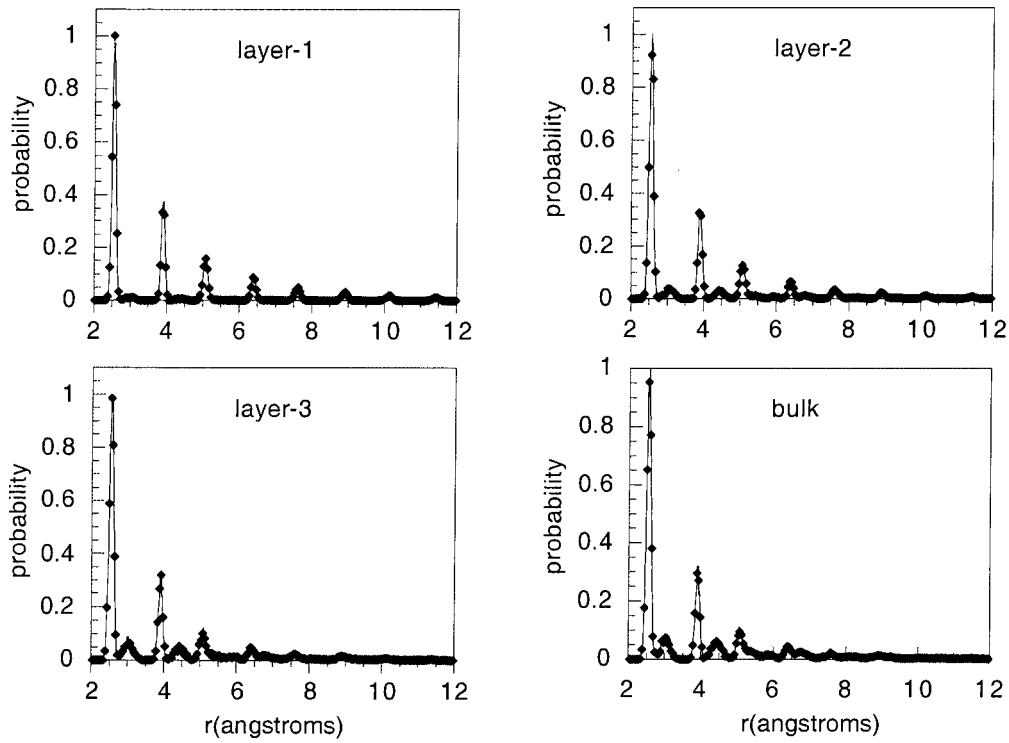

Figure 8. Same as Figure 7, but the surface area of the periodic box is increased to 35 Å × 35 Å.

The r (x, y, z) diffusion of each layer and the corresponding z component should decrease as the size of the alkane chain increases. For the larger alkanes, which have much stronger interactions with the surface, diffusion within the second and third layers may be more strongly influenced by the surface than it is for the smaller alkanes. From such simulations, it may be possible to develop relationships for the diffusion within each layer as a function of temperature and size of the alkane chain.

D. Variations in the Liquid−Surface Interaction Potential. As discussed above in section II, there is some uncertainty in the strength of the potential between the alkane chains and the aluminum cations and oxygen anions of the alumina surface. In addition, these potentials are modified by the use of the r_c cutoff in the Lennard-Jones terms. To determine the effect of these potentials on the interfaces studied here, simulations were run with the ϵ values for the $CH_2(CH_3)\cdots$Al and $CH_2(CH_3)\cdots$O interactions reduced to 43% and 21% of their values in Table 2. These two adjusted potentials give nearly identical density profiles for each of the three alkanes. The density profiles for the 21% adjusted potential are shown in Figure 9, where they are compared with the density profiles for the unadjusted potential. The principal effect of substantially reducing the interaction between the alkane chain UAs and the Al and O atoms of the surface is to decrease the height of the first peak in the density profile, indicating reduced adsorption of the chains on the surface. The effect of the reduced interaction potential is small for the second and subsequent layers. For these model systems, the surface exerts a direct influence on the density of only the first contact liquid layer, and the extent of this influence is dictated by the strength of the surface−liquid interaction potential.

V. Summary

Molecular dynamics simulations are used to study the structure of interfaces resulting from liquid *n*-octane, *n*-hexadecane, and *n*-dotriacontane interacting with a hydroxylated α-Al_2O_3(0001) surface. The simulations are based on well-tested intramolecular and intermolecular potentials for the alkanes and a potential between alkanes and α-Al_2O_3(0001) that was developed previously from high-level ab initio electronic structure theory calculations. The calculated density profiles of the liquid alkanes above the surface show an oscillatory decay to the bulk density. There are five distinguishable layers in this interface, and the densities and structures associated with this layering are remarkably independent of the chain length.

The overall structure of the interface is not strongly dependent on the strength of the interaction potential between the alkane molecules and the surface. Substantial weakening of this potential decreases the density of the innermost layer in direct contact with the surface but has a negligible effect on the density of the remaining layers. The overall interfacial structure is apparently robust with respect to fine details of the interfacial potential.

The simulations suggest that the properties of the innermost layer become more "solidlike", with a more predominant trans structure and fewer gauche defects, as the size of the alkane chain increases. For large alkanes, this property may extend to the second and possibly third layers. Much larger molecular dynamics simulations than those reported here, which use perodic boxes of sufficient size to hold the alkanes, will be required to study this effect in detail.

For the 500 ps time scale reported here, negligible diffusion occurred out of the innermost layer, which contrasts with the considerable diffusion within the layer. Diffusion within the third layer was essentially the same as that for the bulk, while diffusion within the second layer was intermediate between the diffusion of the innermost layer and that of the bulk. For large alkanes, which have a strong interaction with the hydroxylated alumina surface, the presence of the surface may also affect diffusion within the third layer.

Finally, the simulations reported here are based on a united-atom (UA) model for the CH_3 and CH_2 groups of the alkane chains and the OH groups of the hydroxylated alumina surface. This is a widely used model,[83] and because of the removal of

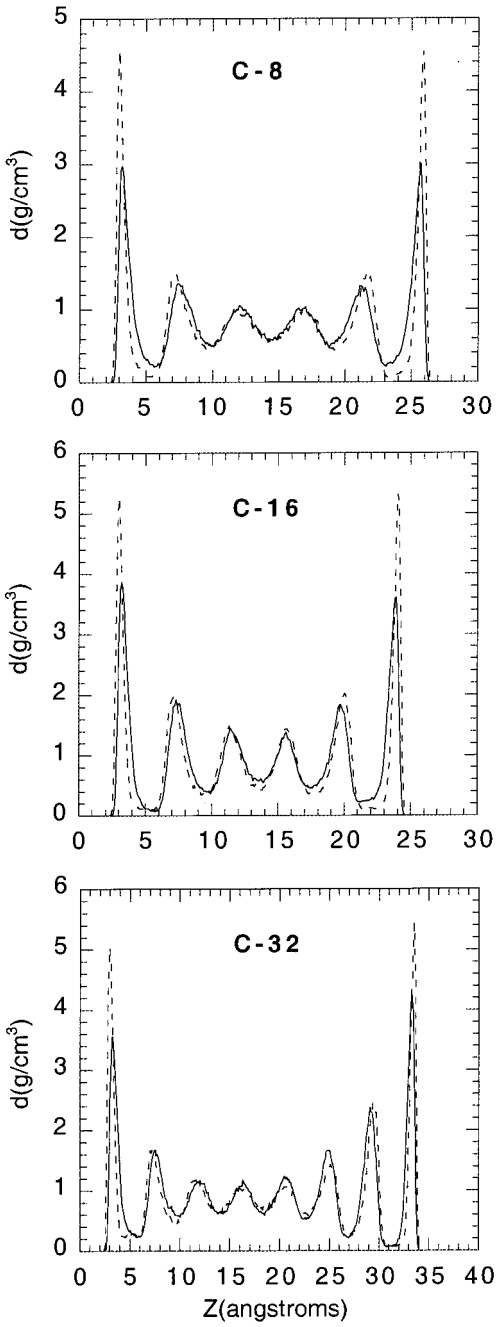

Figure 9. Density profiles at 300 K for interfaces of C8, C16, and C32 liquids with the hydroxylated α-Al_2O_3(0001) surface as a function of the alkane/surface interaction potential. The Lennard-Jones ϵ parameters for the interactions of the $CH_2(CH_3)$ UA with the Al and O surface atoms are the values in Table 2 for the dashed line and 21% of these values for the solid line. The same periodic box was used as in Figure 3.

the high-requency modes and the reduction in the number of atoms, it allows one to simulate larger systems for longer times. However, there is no guarantee that a UA model can properly describe all of the structural and dynamical properties of a molecular system.[41,84−87] In a recent comparison of explicit and united-atom models for alkane chains physisorbed on aluminum-terminated α-Al_2O_3(0001),[41] the UA model properly described the interfacial structure and the trans ↔ gauche interconversion of the alkane chains, but overestimated the diffusion and rotational relaxation of the alkane by approximately a factor of two. This result, as well as those from other studies,[84−87] suggests that some caution must be taken when assessing results from UA simulations, particularly those for dynamical attributes.

Acknowledgment. This research was supported by the Ford Motor Company and the Office of Naval Research. The authors are grateful to Dr. Vipin Chaudhary for the use of computing facilities, Dr. William L. Jorgensen for furnishing the OPLS force field, and David Mann for assisting in the construction of the simulation cell.

References and Notes

(1) Gitzen, W. H. *Alumina as a Ceramic Material*; American Ceramic Society: Columbus, OH, 1970.
(2) Dörre, E.; Hübner, H. *Alumina: Processing, Properties, and Applications*; Springer Publishing: Berlin, Germany, 1984.
(3) Knözinger, H.; Ratnasamy, P. *Catal. Rev. Sci. Eng.* **1978**, *17*, 31.
(4) Zecchina, A.; Coluccia, S.; Morterra, C. *Appl. Spectrosc. Rev.* **1985**, *21*, 259.
(5) Zecchina, A.; Otero Arean, C. *Catal. Rev. Sci. Eng.* **1993**, *35*, 261.
(6) Gonzalez, R. D.; Miura, H. *Catal. Rev. Sci. Eng.* **1994**, *36*, 145.
(7) Laredo, D.; McCrorie, J. D., III; Vaughn, J. K.; Netzer, D. W. *J. Propul. Power* **1994**, *10*, 410.
(8) McHale, J. M.; Navrotsky, A.; Perrotta, A. J. *J. Phys. Chem. B* **1997**, *101*, 603.
(9) McHale, J. M.; Auraux, A.; Perrotta, A. J.; Navrotsky, A. *Science* **1997**, *277*, 788.
(10) Elam, J. W.; Nelson, C. E.; Cameron, M. A.; Tolbert, M. A.; George, S. M. *J. Phys. Chem. B* **1998**, *102*, 7008.
(11) Nelson, C. E.; Elam, J. W.; Cameron, M. A.; Tolbert, M. A.; George, S. M. *Surf. Sci.* **1998**, *416*, 341.
(12) Slayton, R.; Aubuchon, C. M.; Camis, T. L.; Noble, A. R.; Tro, N. J. *J. Phys. Chem.* **1995**, *99*, 2151.
(13) Nishimura, S. Y.; Gibbons, R. F.; Tro, N. J. *J. Phys. Chem. B* **1998**, *102*, 6831.
(14) Katter, U. J.; Hill, T.; Risse, T.; Schlienz, H.; Beckendorf, M.; Klüner, T.; Hamann, H.; Freund, H.-J. *J. Phys. Chem. B* **1997**, *101*, 552, 3776.
(15) Slavav, S. V.; Sanger, A. R.; Chuang, K. T. *J. Phys. Chem. B* **1998**, *102*, 5475.
(16) Lyth, E.; Ng, L. M. *J. Phys. Chem.* **1995**, *99*, 17615. Meyers, J. M.; Desrosiers, R. M.; Cornaglia, L.; Gellman, A. J. *Tribol. Lett.* **1998**, *4*, 155.
(17) Dai, Q.; Robinson, G. N.; Freedman, A. *J. Phys. Chem. B* **1997**, *101*, 4940.
(18) Robinson, G. N.; Dai, Q.; Freedman, A. *J. Phys. Chem. B* **1997**, *101*, 4947.
(19) Coustet, V.; Jupille, J. *Surf. Sci.* **1994**, *307−309*, 1161; *Surf. Interface Anal.* **1994**, *22*, 280.
(20) Coustet, V.; Jupille, J. *Nuovo Cimento* **1997**, *19*, 1657.
(21) Xu, Z.; Ducker, W.; Israelachvili, J. N. *Langmuir* **1996**, *12*, 2263.
(22) Berman, A.; Steiberg, S.; Campbell, S.; Ulman, A.; Israelachvili, J. N. *Tribol. Lett.* **1998**, *4*, 43.
(23) Alvarez, L. J.; Fernández Sanz, J.; Capitán, M. J.; Odriozola, J. A. *Chem. Phys. Lett.* **1992**, *192*, 463.
(24) Blonski, S.; Garofolini, S. H. *Surf. Sci.* **1993**, *295*, 263.
(25) Matsui, M. *Mineral. Mag.* **1994**, *58A*, 571.
(26) Streitz, F. H.; Mintmire, J. W. *Compos. Interfaces* **1994**, *2*, 473; *Phys. Rev. B* **1994**, *50*, 11996.
(27) Blonski, S.; Garofalini, S. H. *Chem. Phys. Lett.* **1993**, *211*, 575.
(28) Blonski, S.; Garofalini, S. H. *Catal. Lett.* **1994**, *25*, 325.
(29) Alvarez, L. J.; León, L. E.; Fernández Sanz, J.; Capitán, M. J.; Odriozola, J. A. *Phys. Rev. B* **1994**, *50*, 2561; *Surf. Sci.* **1995**, *322*, 185; *J. Phys. Chem.* **1995**, *99*, 17872.
(30) Blonski, S.; Garofalini, S. H. *J. Phys. Chem.* **1996**, *100*, 2201.
(31) Streitz, F. H.; Mintmire, J. W. *Langmuir* **1996**, *12*, 4605.
(32) de Sainte Claire, P.; Hass, K. C.; Schneider, W. F.; Hase, W. L. *J. Chem. Phys.* **1997**, *106*, 7331.
(33) Ahuja, R.; Belonoshko, A. B.; Johansson, B. *Phys. Rev. E* **1998**, *57*, 1673.
(34) Alvarez, L. J.; Blumenfeld, A. L.; Fripiat, J. J. *J. Chem. Phys.* **1998**, *108*, 1724.
(35) Holubka, J. W.; Dickie, R. A.; Cassatta, J. C. *J. Adhes. Sci. Technol.* **1992**, *6*, 243.
(36) Godin, T. J.; La Femina, J. P. *Phys. Rev. B* **1994**, *49*, 7691.
(37) Manassidis, I.; Gillan, M. J. *J. Am. Ceram. Soc.* **1994**, *77*, 335.
(38) Hass, K. C.; Schneider, W. F.; Curioni, A.; Andreoni, W. *Science* **1998**, *282*, 265.
(39) Puchin, V. E.; Gale, J. D.; Shluger, A. L.; Kotomin, E. A.; Günster, J.; Brause, M.; Kempter, V. *Surf. Sci.* **1997**, *370*, 190.

(40) Wittbrodt, J. M.; Hase, W. L.; Schlegel, H. B. *J. Phys. Chem. B* **1998**, *102*, 6539.
(41) Bolton, K.; Bosio, S. B. M.; Hase, W. L.; Schneider, W. F.; Hass, K. C. *J. Phys. Chem. B* **1999**, *103*, 3885.
(42) Sawilowsky, E. F.; Schlegel, H. B.; Hase, W. L. *J. Phys. Chem. B*, submitted for publication.
(43) Kramarenko, E. Y.; Winkler, R. G.; Khalatur, P. G.; Khokhlov, A. R.; Reineker, P. *J. Chem. Phys.* **1996**, *104*, 4806.
(44) Balasubrmanian, S.; Klein, M. L.; Siepmann, J. I. *J. Phys. Chem.* **1996**, *100*, 11960; *J. Chem. Phys.* **1995**, *103*, 3184.
(45) Wang, J.; Fichthorn, K. A. *J. Chem. Phys.* **1998**, *108*, 1653.
(46) Christenson, H. K.; Gruen, D. W. R.; Horn, R. G.; Israelachvili, J. N. *J. Chem. Phys.* **1987**, *87*, 1834.
(47) Israelachvili, J. N.; Kott, S. J. *J. Chem. Phys.* **1988**, *88*, 7162.
(48) Israelachvili, J. N.; McGuiggan, P. M.; Homola, A. M. *Science* **1988**, *240*, 190.
(49) Gee, M. L.; McGuiggan, P. M.; Israelachvili, J. N.; Homola, A. M. *J. Chem. Phys.* **1990**, *93*, 1895.
(50) Granick, S. *Science* **1991**, *253*, 1374.
(51) Musil, H.; Herminghaus, S.; Leiderer, P. *Surf. Sci. Lett.* **1993**, *294*, 919.
(52) Klein, J.; Kumacheva, E. *J. Chem. Phys.* **1998**, *108*, 6996.
(53) Kumacheva, E.; Klein, J. *J. Chem. Phys.* **1998**, *108*, 7010.
(54) Schoen, M.; Diestler, D. J.; Cushman, J. H. *J. Chem. Phys.* **1987**, *87*, 5464.
(55) Thompson, P. A.; Robbins, M. O. *Science* **1990**, *250*, 792.
(56) Evens, R. *J. Phys.: Condens. Matter* **1990**, *2*, 8989.
(57) Bitsanis, I. A.; Hadziioannou, G. *J. Chem. Phys.* **1990**, *92*, 3827.
(58) Vacatello, M.; Yoon, D. Y.; Laskowski, B. C. *J. Chem. Phys.* **1990**, *93*, 779.
(59) Thompson, P. A.; Grest, G. S.; Robbins, M. O. *Phys. Rev. Lett.* **1992**, *23*, 3448.
(60) Winkler, R. G.; Matsuda, T.; Yoon, D. Y. *J. Chem. Phys.* **1993**, *98*, 729.
(61) Padilla, P.; Toxvaerd, S. *J. Chem. Phys.* **1994**, *101*, 1490.
(62) Bhushan, B.; Israelachvili, J. N.; Landman, U. *Nature* **1995**, *373*, 607.
(63) Ballamudi, R. K.; Bitsanis, I. A. *J. Chem. Phys.* **1996**, *105*, 7774.
(64) Dijkstra, M. *J. Chem. Phys.* **1997**, *107*, 3277.
(65) Gao, J.; Luedtke, W. D.; Landman, U. *J. Phys. Chem. B* **1997**, *101*, 4013.
(66) Gao, J.; Luedtke, W. D.; Landman, U. *J. Chem. Phys.* **1997**, *106*, 4309.
(67) Koieke, A.; Yoneya, M. *J. Phys. Chem. B* **1998**, *102*, 3669.
(68) Toxvaerd, S. *J. Chem. Phys.* **1981**, *74*, 1998.
(69) Magda, J. J.; Tirrell, M.; Davis, H. T. *J. Chem. Phys.* **1985**, *83*, 1888.
(70) *Cerius*^{2}; BIOSYM/Molecular Simulations: San Diego, CA, 1995.
(71) Taken from the crystal database of *Cerius*^{2} with lattice parameters of $a = 4.748$ and $c = 12.954$ and Al−O distances of 1.8524 and 1.9628 Å.
(72) Allen, M. P.; Tildesley, D. J. *Computer Simulation of Polymers*; Clarendon Press: Oxford, U.K., 1989.
(73) Jin, R. Y.; Boyd, R. H. *J. Chem. Phys.* **1998**, *108*, 9912.
(74) Boyd, R. H.; Gee, R. H.; Han, J.; Jin, R. Y. *J. Chem. Phys.* **1994**, *101*, 788.
(75) Takeuchi, H.; Roe, R.-J. *J. Chem. Phys.* **1991**, *94*, 7446.
(76) Smith, G. D.; Yoon, D. Y.; Zhu, W.; Ediger, M. D. *Macromolecules* **1994**, *27*, 5563.
(77) Jogensen, W. L.; Maxwell, D. S.; Tirado-Rives, J. *J. Am. Chem. Soc.* **1996**, *118*, 11225. Kaminski, G.; Duffy, E. M.; Matsui, T.; Jorgensen, W. L. *J. Phys. Chem.* **1994**, *98*, 13077. Jorgensen, W. L.; Madura, J. D.; Swenson, C. J. *J. Am. Chem. Soc.* **1984**, *106*, 6638. Jorgensen, W. L. *J. Phys. Chem.* **1986**, *90*, 1276.
(78) Ahn, J.; Rabalais, J. W. *Surf. Sci.* **1997**, *388*, 121.
(79) Mansfield, K. F.; Theodorou, D. N. *Macromolecules* **1991**, *24*, 4295.
(80) Berendsen, H. J. C.; Postma, J. P. M.; van Gunsteren, W. F.; DiNola, A.; Haak, J. R. *J. Chem. Phys.* **1984**, *66*, 2821.
(81) Swope, W. C.; Andersen, H. C.; Berens, P. H.; Wilson, K. R. *J. Chem. Phys.* **1982**, *76*, 637.
(82) Gee, M. L.; Israelachvili, J. N. *J. Chem. Soc., Faraday Trans.* **1990**, *86*, 4049.
(83) See, for example, refs 44, 45, and 63−66.
(84) Krishna Pant, P. V.; Boyd, R. H. *Macromolecules* **1992**, *25*, 494. Krishna Pant, P. V.; Han, J.; Smith, G. D.; Boyd, R. H. *J. Chem. Phys.* **1993**, *99*, 597.
(85) Toxvaerd, S. *J. Chem. Phys.* **1990**, *93*, 4290. Padilla, P.; Toxvaerd, S. *J. Chem. Phys.* **1991**, *94*, 5650.
(86) Smith, G. D.; Yoon, D. Y. *J. Chem. Phys.* **1994**, *100*, 649.
(87) McCoy, J. D.; Mateas, S.; Zorlu, M.; Curro, J. G. *J. Chem. Phys.* **1995**, *102*, 8635.